LBL--32311

DE93 004716

MECHANICS AND MECHANISMS OF CYCLIC FATIGUE-CRACK PROPAGATION IN TRANSFORMATION-TOUGHENED ZIRCONIA CERAMICS

M. J. Hoffman,[1,2] R. H. Dauskardt,[1] Y.-W. Mai,[2] and R. O. Ritchie[1]

[1]Center for Advanced Materials, Materials Sciences Division
Lawrence Berkeley Laboratory
and
Department of Materials Science and Mineral Engineering
University of California, Berkeley, CA 94720

[2]Center for Advanced Materials Technology, Department of Mechanical Engineering
University of Sydney, Sydney, N.S.W. 2006, Australia

May 1992

to be presented at
The Fifth International Conference on the Science and Technology of Zirconia,
Zirconia V, "AUSTCERAM 92," Melbourne, Australia, August 1992

This work was supported by the Director, Office of Energy Research, Office of Basic Energy Sciences, Materials Sciences Division of the U.S. Department of Energy under Contract No. DE-AC03-79SF00098-1049.

MECHANICS AND MECHANISMS OF CYCLIC FATIGUE-CRACK PROPAGATION IN TRANSFORMATION-TOUGHENED ZIRCONIA CERAMICS

M. J. Hoffman,[1,2] R. H. Dauskardt,[1] Y.-W. Mai,[2] and R. O. Ritchie[1]

[1]Center for Advanced Materials, Materials Sciences Division, Lawrence Berkeley Laboratory, and Department of Materials Science and Mineral Engineering
University of California, Berkeley, CA 94720
[2]Center for Advanced Materials Technology, Department of Mechanical Engineering
University of Sydney, Sydney, N.S.W. 2006, Australia

ABSTRACT

Damage and cyclic fatigue failure under alternating loading in transformation-toughened zirconia ceramics is reviewed and compared to corresponding behavior under quasi-static loading (static fatigue). Current understanding of the role of transformation toughening in influencing cyclic fatigue-crack propagation behavior is examined based on studies which altered the extent of the tetragonal-to-monoclinic phase transformation in Mg-PSZ through sub-eutectoid aging. These studies suggest that near-tip computations of the crack-driving force (in terms of the *local* stress intensity) can be used to predict crack-growth behavior under constant amplitude and variable-amplitude (spectrum) loading, using spatially resolved Raman spectroscopy to measure the extent of the transformation zones. In addition, results are reviewed which rationalize distinctions between the crack-growth behavior of pre-existing, "long" (> 2 mm), through-thickness cracks and naturally-occurring, "small" (1 to 100 μm), surface cracks in terms of variations in crack-tip shielding with crack size. In the present study, the effect of grain size variations on crack-growth behavior under both monotonic (R-curve) and cyclic fatigue loading are examined. Such observations are used to speculate on the mechanisms associated with cyclic crack advance, involving such processes as alternating shear via transformation-band formation, cyclic modification of the degree of transformation toughening, and uncracked-ligament (or grain) bridging.

INTRODUCTION

Ceramic materials in their traditional sense have always been thought of as brittle in nature, displaying purely linear elastic deformation behavior; correspondingly, lifetime prediction for ceramic components subjected to cyclic loads are generally based upon the cumulative time under static loading. The development of toughened ceramics designed for use in structural applications, however, relies on energy dissipating processes associated with nonlinear constitutive behavior. These processes result in toughening from fiber and whisker reinforcement, phase-transformation and microcracking, crack deflection, and crack bridging,

all crack-tip shielding mechanisms which primarily act behind the crack tip and induce crack-resistance or rising R-curve behavior [1].

In addition to R-curve behavior, toughened ceramics have been shown to suffer mechanical damage under cyclic loading [e.g., 2-18], despite initial claims to the contrary [19]. Consequently, lifetimes are lower than those predicted by simply integrating the effects of environmental damage or static fatigue. While detailed models of the crack-advance mechanisms are currently unclear, preliminary observations [9,12,16,17] suggest that cyclic fatigue is motivated by a suppression of crack-tip shielding. For example, in monolithic ceramics such as coarse-grained alumina, where toughening is promoted by crack bridging from interlocking grains, the grain bridges can be degraded under cyclic loading due to wear processes from repeated sliding of the interfaces. For many ceramic materials, however, such as transformation-toughened zirconias, the microstructural mechanisms of cyclic fatigue damage remain uncertain.

The objective of this paper is to review what is known about fatigue failure in transformation-toughened zirconia ceramics, with specific reference to partially stabilized zirconia (PSZ). In these materials, toughening can occur from the *in situ* stress-induced martensitic transformation of the tetragonal zirconia phase to the monoclinic phase in the vicinity of the crack tip; this phase change involves a ~4% dilation and a small degree of shear strain (~16%) [20-22]. In simple terms, toughening then results as the crack grows into the zone of transformed material, which exerts compressive forces on the crack surfaces, consequently shielding the crack tip from the applied stresses and leading to R-curve behavior (Fig. 1).

CYLIC FATIGUE BEHAVIOR

Stress/Life Data

Several studies using stress/life (S/N) testing have confirmed that cyclic loads lead to a degradation in strength in PSZ [e.g., 4,8,11,18]. Fig. 2, for example, shows failure data in

Mg-PSZ from bend samples where cracking was initiated from microhardness indents [18]. Lifetimes for statically loaded samples can be seen to markedly exceed those obtained under cyclic loading; moreover, as the lifetimes of cyclically loaded samples are significantly less than those predicted from static fatigue models, it is clear that PSZ shows true cyclic fatigue degradation.

Under cyclic loading, there is clear evidence for many ceramics that lifetimes in smooth-bar S/N tests under tension-compression (R = -1) loads are distinctly lower than corresponding tests under tension-tension (R > 0) loads [4,15]. For Mg-PSZ, this appears to result from the more damaging nature of fully reversed loads in promoting crack initiation as microcrack densities are observed to be far higher after cycling at R = -1 compared to R = 0 [15].

Crack-Propagation Data: Long Cracks

The most persuasive evidence for cyclic fatigue degradation, however, has resulted from studies on subcritical crack growth obtained under cyclic loading conditions on "long" (> 2 mm) through-thickness cracks in compact-tension samples of MS-grade Mg-PSZ (Fig. 3a) [2,7]. Crack-growth rate data (Fig. 4) are several orders of magnitude faster than data generated under constant loading (static fatigue) conditions at the same (applied) maximum stress intensity (K_{max}); moreover, the threshold stress intensity for crack growth is over 40% lower under cyclic loads. Such crack-growth behavior is considered to be truly cyclic in nature, as shown by experiments involving monitoring growth rates at constant K_{max} with varying K_{min} [2].

Effects of Temperature and Environment

Although data are relatively scarce, cyclic fatigue behavior in zirconia ceramics is sensitive to the environment. Cyclic crack-growth rates, shown in Fig. 5 for AF-grade Mg-PSZ, display a progressive acceleration of water compared to moist air and dry gaseous nitrogen [7]. Environmental effects have also been observed in rotational fatigue S/N data for

PSZ tested in aqueous solutions of HCl and NaOH [4]; these results further indicate that cyclic fatigue lifetimes in PSZ decrease significantly with increasing temperature between 20 and 600°C.

Influence of Transformation Toughening

The degree of crack-tip shielding, specifically from transformation toughening, can also have a significant effect of cyclic crack-growth rates [7]. Microstructures with larger crack-tip transformation zones, which display steeply rising R-curves and high toughness values, are found to show the highest resistance to cyclic crack growth, as shown by the steady-state crack-growth rate vs. applied stress-intensity range (ΔK) data in Fig. 6a for Mg-PSZ, sub-eutectoid aged to differing K_c toughnesses between 2.9 and 15.5 MPa$\sqrt{m}$. In general terms, growth rates (da/dN) appear to follow a simple Paris power-law:

$$da/dN = C \Delta K^m \quad , \tag{1}$$

where the applied $\Delta K = K_{max} - K_{min}$, and C and m are experimentally determined scaling constants. Note that values of the exponent m in Mg-PSZ range between 21 and 42, values that are far higher than those typically reported for metals.

The effect of microstructure seen in Fig. 6a can be rationalized in terms of the effect of the crack-tip shielding on the local (near-tip) stress intensity, ΔK_{tip}, which drives the crack [7]:

$$\Delta K_{tip} = K_{max} - K_s \quad , \tag{2}$$

where the shielding stress intensity, K_s, due to a fully developed steady-state dilatant transformed zone of width w, is given in terms of the dilatational component of the transformation strain, ϵ^T (~4%), and the volume fraction of transforming phase, f, as [23]:

$$K_s = \alpha E' \epsilon^T f w^{1/2} \quad . \tag{3}$$

E' is the effective Young's modulus and α is constant that depends upon frontal zone shape

(= 0.22 for a hydrostatic stress-field transformation zone and 0.25 for the more semicircular profiles observed in higher toughness Mg-PSZ microstructures [24]). Using Raman spectroscopy to determine the size and shape of the transformation zone surrounding the crack, values of the near-tip stress-intensity range can be computed from Eqs. 2 & 3; by characterizing the crack-growth rate data in terms of ΔK_{tip}, rather than the applied ΔK, crack-growth behavior for the four microstructures can be normalized (Fig. 6b) [7]. This implies that the effect of transformation shielding on fatigue-crack growth is essentially identical to its effect on steady-state fracture toughness, i.e., transformation shielding reduces the effective stress intensity actually experienced at the crack tip.

Variable Amplitude Loading

The phase transformation in PSZ also has a significant impact on transient fatigue-crack propagation behavior under variable-amplitude loading [10,11]; examples of the effect of load history on crack-growth rates are shown in Fig. 7 for MS and TS grades of Mg-PSZ [10]. Similar to behavior in metals, high-low block loading and single tensile overloads result in a transient retardation, whereas low-high block loading results in a transient acceleration. Relatively accurate predictions of the post load-change growth rates have been made by computing the extent of crack-tip shielding in the changing transformation zone following the load changes; these predictions are shown by the dotted lines in Fig. 7a [10]. The varying size of the transformation zone is measured using spatially-resolved Raman spectroscopy; zone sizes for the loading sequence shown in Fig. 7b are plotted in Fig. 8, where it is clear that changes in load significantly affect the degree of phase transformation at the crack tip. Note that significant variations in growth rates are apparent for relatively small changes in ΔK; this follows because of the steep slope of the da/dN-ΔK curves found in ceramics.

Two models have been developed to predict the effects of variable-amplitude loading in PSZ. One idealizes the transformed zones as a series of steady-state zones with a width depending on the level of applied stress intensity [10]; the other considers a hydrostatic stress

profile to cause the transformation to predict the wake effect [11]. Both models provide reasonable predictions of transient growth-rate behavior.

Grain Size Effects

Only limited studies have been performed to date on the role of grain size on cyclic fatigue behavior in zirconia ceramics. Shown in Fig. 9 are R-curve and corresponding fatigue-crack propagation data for MS- and TS-grade Mg-PSZ with grain sizes of ~32, 50 and 100 μm. As noted in previous studies [7], the enhanced degree of transformation toughening in the TS-grade promotes both superior toughness and resistance to fatigue-crack growth. Moreover, in general it is apparent that toughness and fatigue resistance are increased with increase in grain size (although the 100-μm MS-grade sample shows a surprisingly low toughness); however, despite differences in their R-curve behavior, fatigue-crack growth rates for 50 and 100 μm microstructures in both MS and TS grades are essentially identical. The reason for such large grain-size effects are as yet uncertain but may be associated with the transformation of large grain-boundary tetragonal particles.

Crack-Propagation Data: Small Cracks

The question of small cracks (of a size approaching microstructural dimensions) is undoubtedly of special concern in ceramics; because of their low toughness, most ceramic components will not be able to tolerate the presence of physically long cracks in service. Such small cracks may be initiated from inherent processing flaws, interfaces between reinforcement and matrix phases, grain boundaries and other defects in the microstructure.

For Mg-PSZ, experimental data have been generated for naturally-occurring small flaws (Fig. 3b) under both static fatigue [25] (Fig. 10a) and cyclic fatigue [15] (Fig. 10b) conditions. In both cases, the slopes of the logarithmic crack velocity vs. applied stress intensity curves appear to be negative; this is in direct contrast to long-crack behavior (e.g., Figs. 5,6) yet consistent with extensive results on small cracks published for metallic materials [e.g., 26]. Moreover, small-crack growth rates can be seen to be far in excess of those of corresponding

long cracks at the same applied stress intensity, and furthermore to occur at applied stress intensities below the long-crack threshold. Although this behavior can be attributed to a number of factors [26], the primary reason is that the extent of crack-tip shielding (in the case of Mg-PSZ from transformation toughening) is diminished with small flaws because of their limited wake. Although the applied stress intensity increases with increase in crack size, the shielding stress intensity is also enhanced as the transformation zone is developed in the crack wake. The near-tip stress intensity which drives the crack (Eq. 2), and hence the crack-growth behavior, is thus the result of a mutual competition between these two factors; initially K_{tip} is diminished with crack extension until a steady-state transformation zone is established, whereupon behavior approaches that of a long crack. Failure ultimately results from the coalescence of such small cracks.

MECHANISMS OF CYCLIC FATIGUE

Detailed models of the crack-advance and microstructural damage mechanisms associated with cyclic fatigue in ceramics are currently not available; such models are integral to material development for optimum fatigue resistance and to the prediction of structural design lifetimes of ceramic components. However, a number of observations have been recently reported for Mg-PSZ which may shed some light on potential mechanisms; these are summarized below.

In situ studies, performed in a scanning electron microscope at temperatures between 20 and 650°C [13], showed that the region of stable crack growth in Mg-PSZ was very limited above ~450°C where cracking was very unstable (presumably due to the lack of appreciable phase transformation). Extrapolation of these results suggested that no subcritical crack growth by fatigue was possible at all above 750-800°C. At 20°C, however, "slip lines", similar to those seen in metal fatigue, were observed to form at the crack tip; a mechanism of crack advance was proposed involving propagation along these slip bands (which contain transformed

precipitates). This mechanism invokes the contentious concept of crack extension in ceramics by alternating crack-tip blunting and resharpening, similar to the well known mechanism for fatigue-crack growth in metallic alloys. Whereas this is unlikely in non-transforming ceramics at ambient temperatures, it is conceivable that transformation-band formation at the crack tip in phase transforming ceramics such as Mg-PSZ may provide a feasible mechanism for blunting; in fact, certain authors [13,14] have reported the formation of fatigue striations on fracture surfaces in Mg-PSZ and Y-TZP.

The phase transformation itself, however, appears to be relatively unaffected by cyclic loads. *In situ* measurements of the morphology and nature of transformation zones in Mg-PSZ using interference microscopy and spatially-resolved Raman spectroscopy (e.g., Fig. 11) indicated no change in zone size surrounding monotonically and cyclically loaded cracks at equivalent stress-intensity levels [7,24,27].

In addition to crack-tip shielding due to the transformation, evidence of uncracked-ligament bridging is prevalent during crack growth in Mg-PSZ (Fig. 12). Under cyclic loading, progressive wear degradation of the bridges may reduce the bridging capacity of the resulting bridging zone thereby exposing the crack tip to an increased driving force. Similar to behavior in metal-matrix composites [28], such uncracked ligaments most likely result from the formation of microcracks *ahead* of the crack tip; this would suggest that crack-tip blunting is occurring under cyclic loading since under these conditions the maximum principal stresses would be located approximately two crack-tip opening displacements ahead of the tip. However, direct observations of blunting in these materials has yet to be made.

Evidence of microcracking during fatigue has been reported for Y-TZP [14], where the compliance of samples loaded uniaxially was observed to increase with cyclic loading due to the formation of microcracks in the bulk of the material. These authors proposed that crack initiation occurs from pre-existing surface or bulk flaws, and that the localized stresses surrounding these flaws promote microcrack nucleation and coalescence; this results in significant strength degradation during cyclic loading. Direct observations of microcracks have

been made in ZTA, Mg-PSZ and Y-TZP using transmission electron microscopy [29]; the origin of this microcracking was attributed to large residual stresses resulting from the martensitic transformation, or to large localized stresses from the elastic anisotropy [30].

CONCLUSIONS

Experimental evidence clearly shows that phase-transforming zirconia ceramics suffer significant strength degradation and premature failure under cyclic loads. The cyclic fatigue damage appears to be motivated by the inelasticity associated with transformation and enhanced microcracking, and results in the subcritical propagation of cracks by an apparently true cyclic fatigue process; the precise micromechanisms of crack advance, however, are as yet undetermined.

A significant amount of this work has centered on the propagation behavior of "long" (> 2 mm) through-thickness cracks in Mg-PSZ. Based on these studies, cyclic crack-growth rates have been found to show a power-law dependence on the stress intensity with an exponent of above 20, and to be sensitive to such variables as load ratio, crack size, temperature and environment, degree of transformation, grain size and loading spectra. In contrast, only limited studies have addressed the question of fatigue-crack initiation in ceramics; many difficulties, however, exist with the reproducibility and analysis of such data suggesting that statistical approaches will be essential for developing engineering design criteria for these materials.

ACKNOWLEDGEMENTS

This work was supported by the Director, Office of Energy Research, Office of Basic Energy Sciences, Materials Sciences Division of the U.S. Department of Energy under Contract No. DE-AC03-76SF00098-1049. The authors would like to thank collaborative studies with Drs. W. C. Carter, D. B. Marshall and D. K. Veirs during the course of this work.

REFERENCES

1. A.G.Evans, in "Fracture Mechanics: Perspectives and Directions", *ASTM STP 1020*, R.P.Wei and R.P.Gangloff, eds., American Society for Testing and Materials, Philadelphia, PA, (1989) pp. 267-91.

2. R.H.Dauskardt, W.Yu and R.O.Ritchie, *J. Am. Ceram. Soc.*, **70** (1987) C248.

3. L.Ewart and S.Suresh, *J. Mater. Sci.* **22** (1987) 1173.

4. M.V.Swain and V.Zelizko, in "Advances in Ceramics, 24B Sci. and Tech. Zirconia III", S.Sõmiya, H.Yamamoto and H.Yanagida, eds., American Ceramic Society, Westerville, OH (1988) pp. 595-606.

5. M.J.Reece, F.Guiu and M.F.R.Sammur, *J. Am. Ceram. Soc.*, **72** (1989) 348.

6. M.Masuda, T.Soma, M.Matsui and I.Oda, *J. Eur. Ceram. Soc.*, **6** (1990) 253.

7. R.H.Dauskardt, D.B.Marshall and R.O.Ritchie, *J. Am. Ceram. Soc.*, **73]** (1990) 893.

8. W.Lentz, Y-W.Mai, M.V.Swain and B.Cotterell, *Proc. AUSTCERAM Conf.*, **90** (1990) pp. 750-53.

9. R.O.Ritchie, R.H.Dauskardt, W.Yu and A.M.Brendzel, *J. Biomed. Mater. Res.*, **24** (1990) 189.

10. R.H.Dauskardt, W.C.Carter, D.K.Veirs and R.O.Ritchie, *Acta metall. mater.*,**38** (1990) 2327.

11. K.Duan, B.Cotterell and Y.-W.Mai, *Proc. Fract. Mechanics of Ceramics Conf.*, Nagoya, Japan, (1991).

12. S.Lathabai, J.Rödel and B.R.Lawn, *J. Am. Ceram. Soc.*, **74** (1991) 1340.

13. D.Davidson, J.B.Campbell and J.Lankford, *Acta metall. mater.*, **39** (1991) 1319.

14. S.-Y. Liu and I-Wei Chen, *J. Am. Ceram. Soc.*, **74** (1991) 1197 and 1206.

15. A.A.Steffen, R.H.Dauskardt and R.O.Ritchie, *J. Am. Ceram. Soc.*, **74** (1991) 1259.

16. F.Guiu, M.J.Reece and D.A.J.Vaughan, *J. Mater. Sci.*, **26** (1991) 3275.

17. X.-Z.Hu and Y.-W.Mai, *J. Am. Ceram. Soc.*, **75** (1992).

18. M.J.Hoffman, W.Lentz, M.V.Swain and Y.W.Mai, *J. Eur. Ceram. Soc.*, 8 (1992) in review.

19. A.G.Evans, *Int. J. Fract.*, **16** (1980) 485.

20. R.H.J.Hannink and M.V.Swain, *J. Aust. Ceram. Soc.*, **18** (1982) 53.

21. R.H.J.Hannink, *J. Mater. Sci.*, **18** (1983) 457.

22. M.S.Dadkhah, D.B.Marshall, W.L.Morris and B.N.Cox, *J. Am. Ceram. Soc.*, **74** (1990) 2939.

23. R.M.McMeeking and A.G.Evans, *J. Am. Ceram. Soc.*, **65** (1982) 242.

24. D.B.Marshall, M.C.Shaw, R.H.Dauskardt, R.O.Ritchie, M.Readey and A.H.Heuer, *J. Am. Ceram. Soc.*, **73** (1990) 2659.

25. D.Jensen, V.Zelizko and M.V.Swain, *J. Mater. Sci. Lett.*, **8** (1989) 1154.

26. S.Suresh and R.O.Ritchie, *Int. Met. Rev.*, **29** (1984) 445.

27. R. H. Dauskardt, D. K. Veirs and R. O. Ritchie, unpublished work, Lawrence Berkeley Laboratory, University of California (1991).

28. J.-K.Shang and R.O.Ritchie, *Metall. Trans. A*, **20A** (1989) 897.

29. A.H.Heuer, M.Rühle and D.B.Marshall, *J. Am. Ceram. Soc.*, **73** (1990) 1084.

30. D.B.Marshall and M.V.Swain, *J. Am. Ceram. Soc.*, **71** (1988) 399.

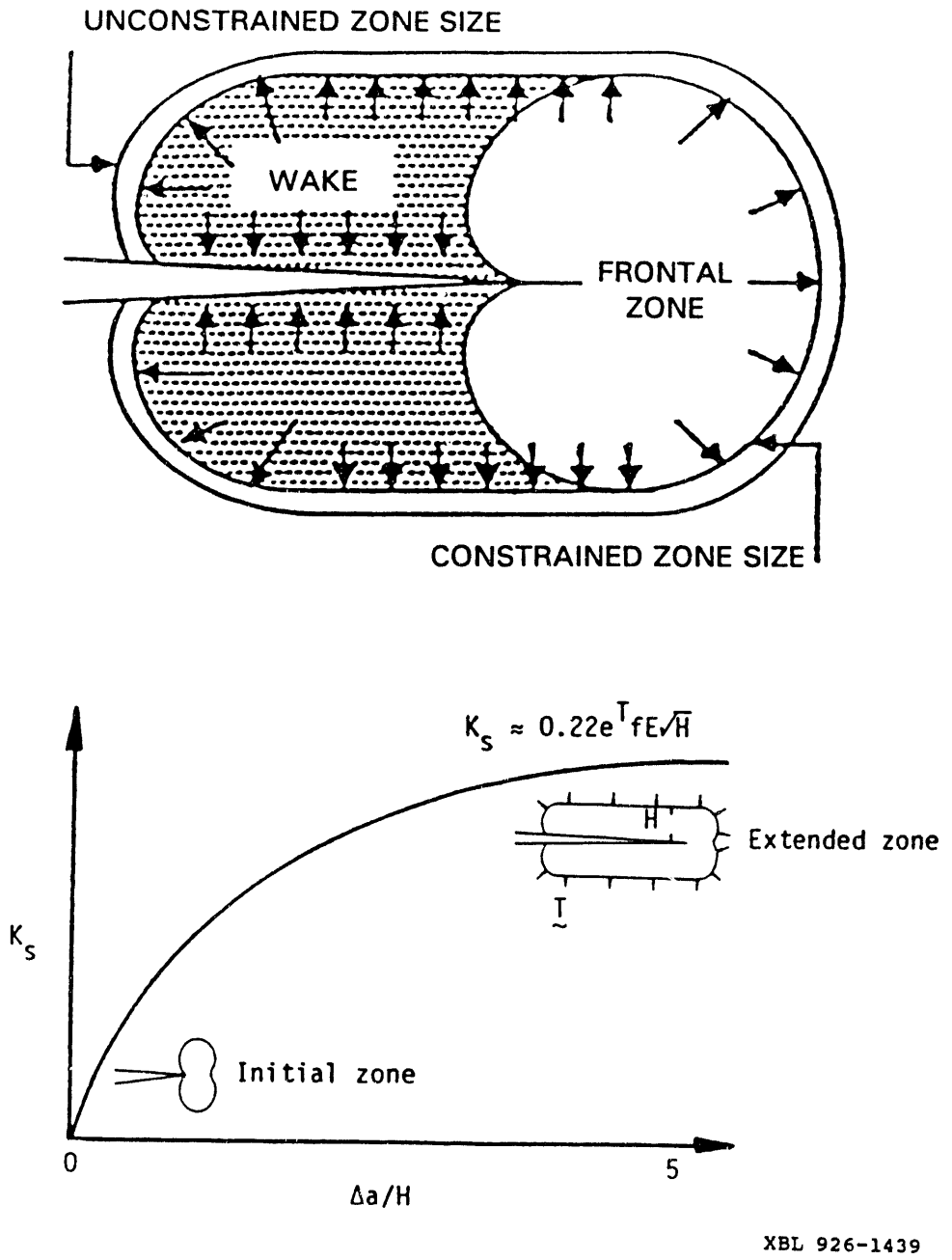

Fig. 1: Schematic illustration of a) the transformation zone surrounding a crack in a phase-transforming ceramic, and b) the resulting resistance curve showing the increase in shielding stress intensity K_s with increasing crack extension ΔK.

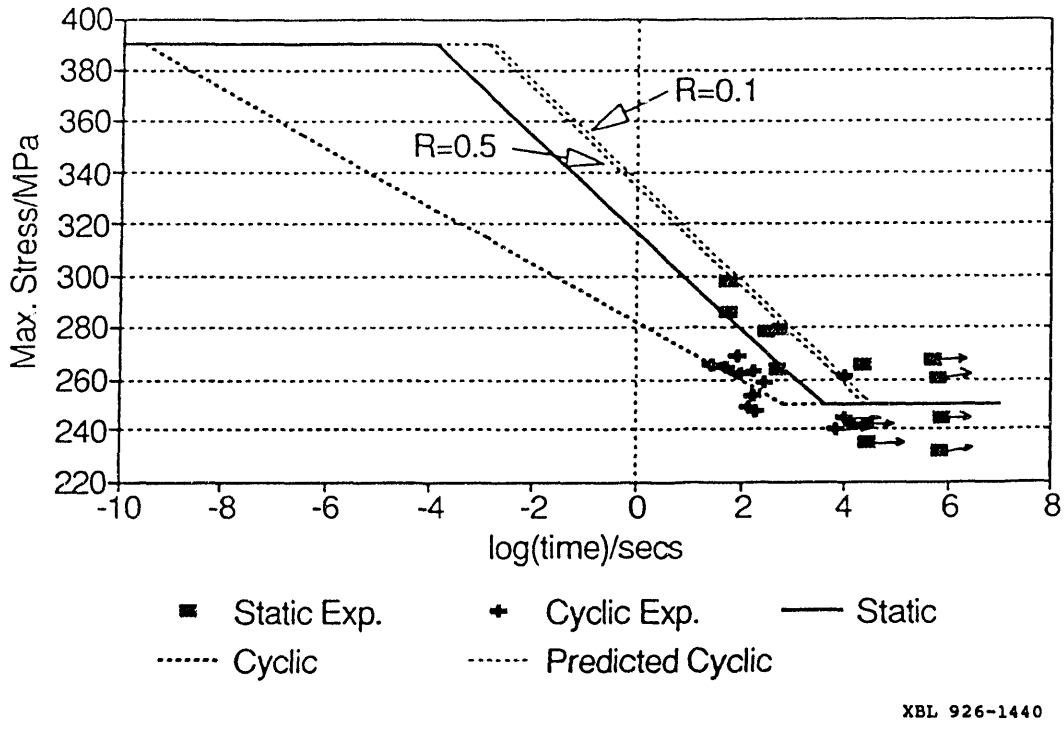

Fig. 2: Stress/life data for MS-grade Mg-PSZ ($K_{I_c} \approx 11.5$ MPa$\sqrt{m}$) under quasi-static and cyclic (R = 0.1 and 0.5) loading, showing a comparison of experimental vs. predicted lifetimes [18].

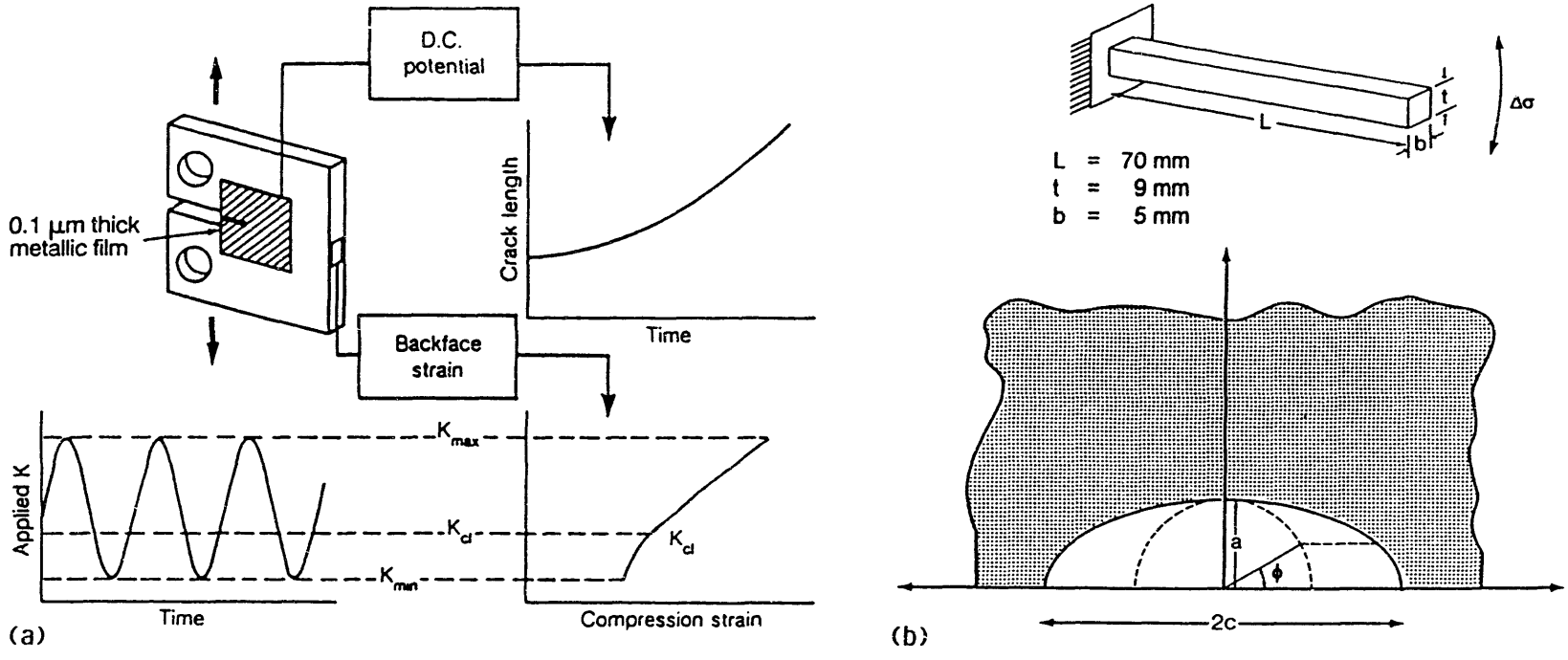

XBL 882-420E

Fig. 3: Experimental techniques used to measure cyclic fatigue-crack growth rates, showing a) compact-tension C(T) specimen and procedures used to monitor crack length and the stress intensity, K_{cl}, at crack closure for "long" cracks, and b) cantilever-bend specimen and semi-elliptical surface crack configuration for tests on small cracks [2,7,15].

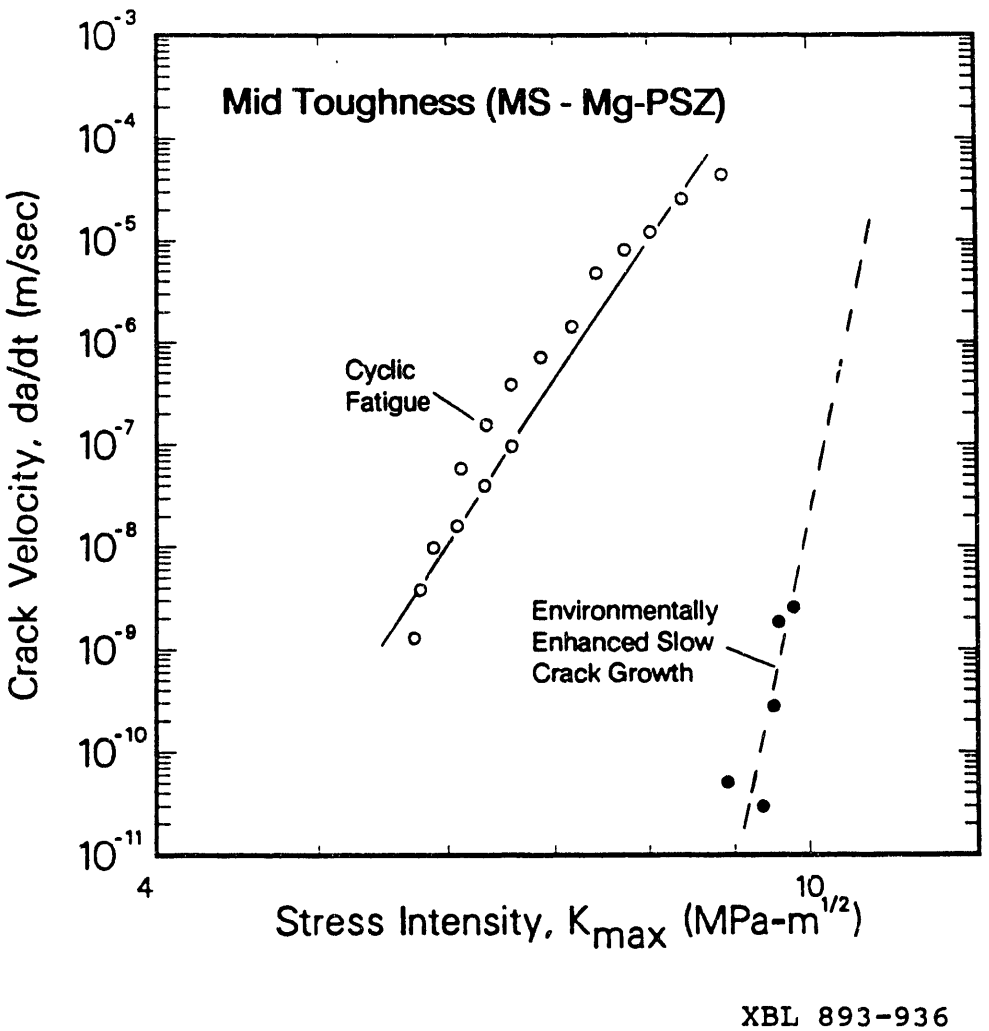

XBL 893-936

Fig. 4: Comparison of the crack velocity vs. maximum stress intensity (K_{max}) curves for static fatigue (slow crack growth) and cyclic fatigue (at R = 0.1) in MS-grade Mg-PSZ in a moist air environment, showing cyclic crack velocities up to 7 orders of magnitude faster at equivalent K_{max} levels [7].

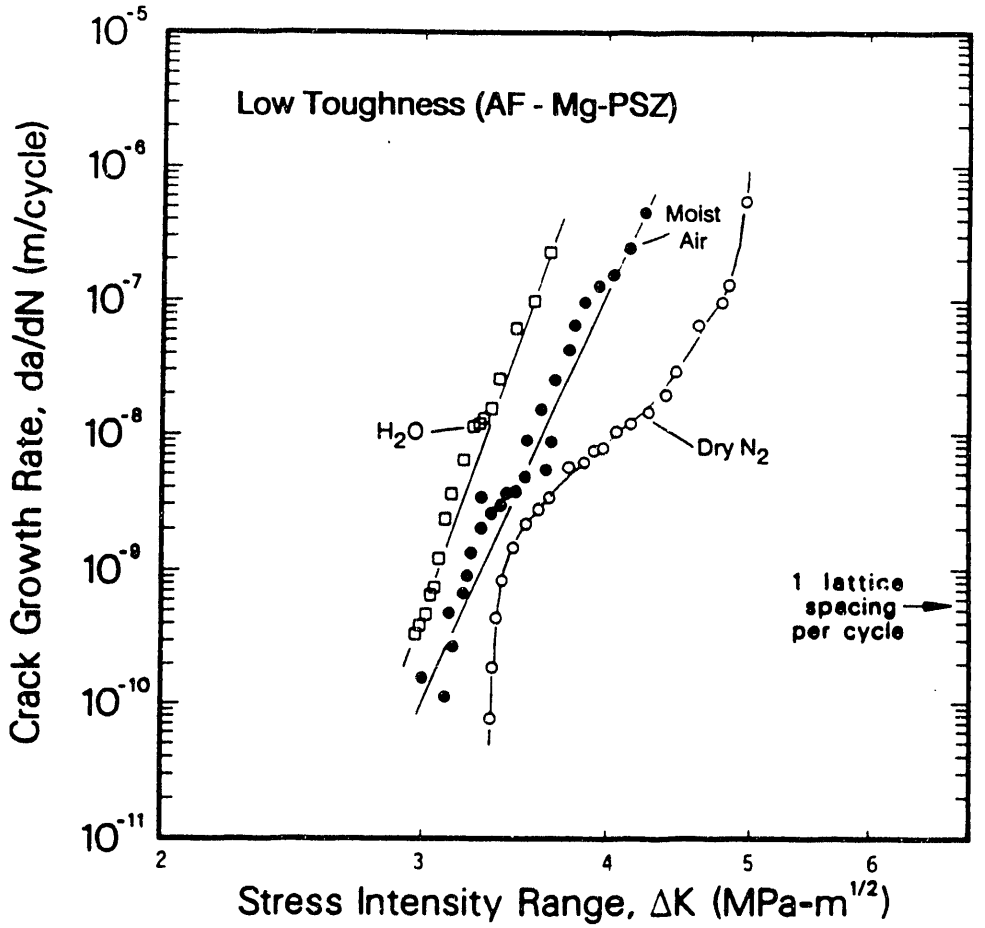

Fig. 5: Cyclic crack-growth rates, da/dN, as a function of the stress-intensity range, ΔK, in AF-grade Mg-PSZ ($K_c \approx 5.5$ MPa$\sqrt{m}$) tested at 50 Hz in long-crack C(T) samples, showing accelerated growth-rate behavior in distilled water and moist air compared to dehumidified gaseous nitrogen [7].

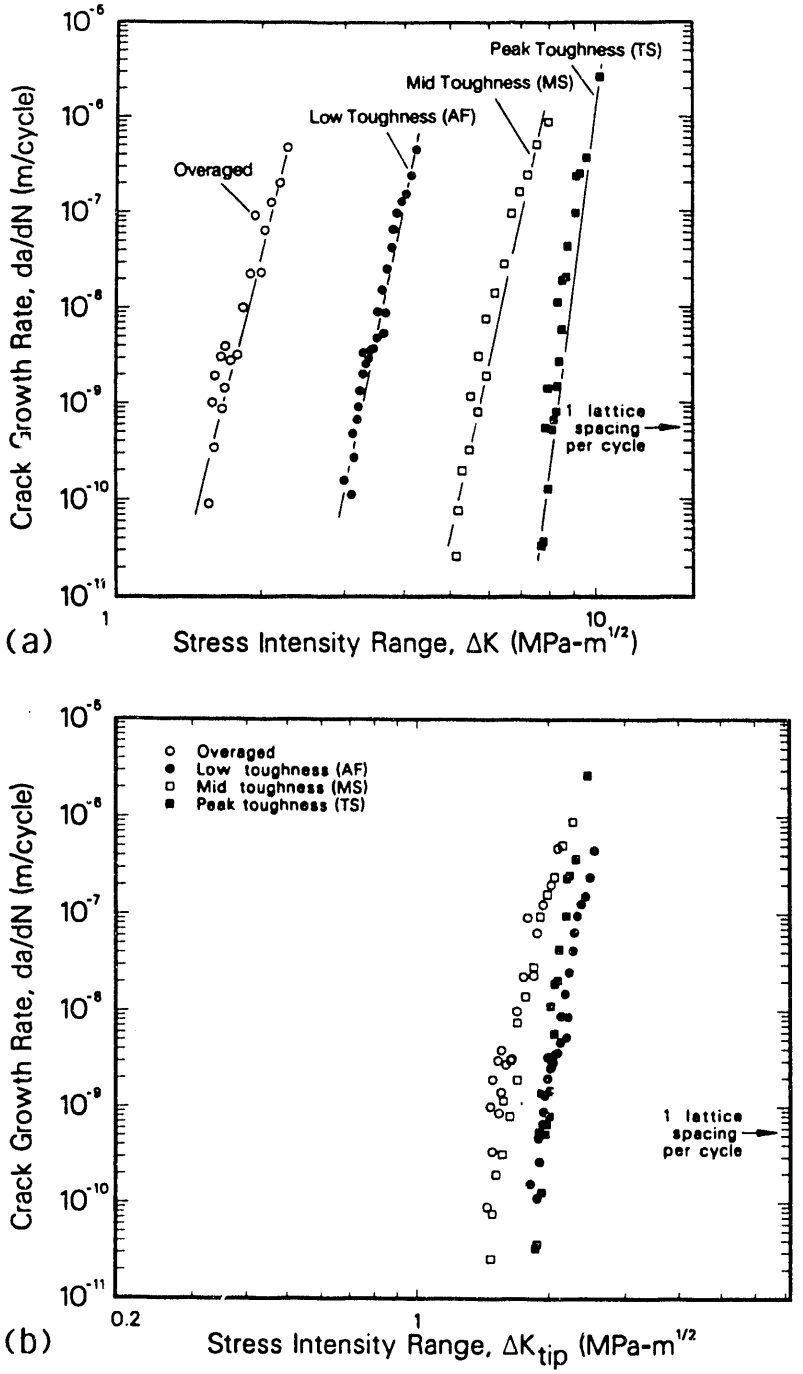

Fig. 6: Long-crack growth-rate data for cyclic fatigue in overaged ($K_c \approx 2.9$ MPa$\sqrt{m}$) and transformation-toughened Mg-PSZ as a function of a) the applied stress-intensity range, $\Delta K = K_{max} - K_{min}$, and b) the near-tip stress-intensity range, $\Delta K = K_{max} - K_s$ [7].

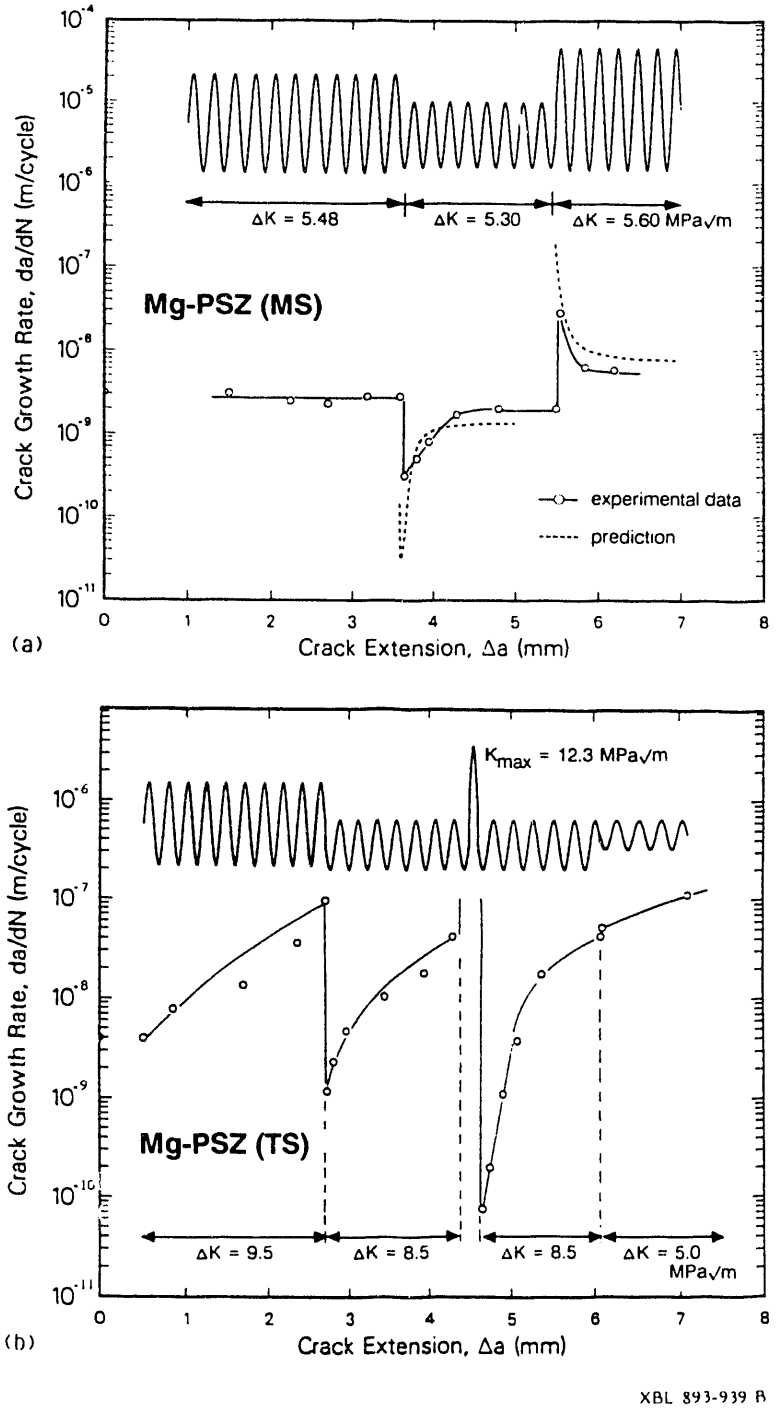

Fig. 7: Transient fatigue-crack growth behavior in a) MS-grade and b) TS-grade Mg-PSZ, showing variation in growth rates following various block loading and tensile overload cycling. Predictions in a) rely on steady-state crack-growth rate data (Fig. 6b) and transformation-zone size measurements (Fig. 8) [10].

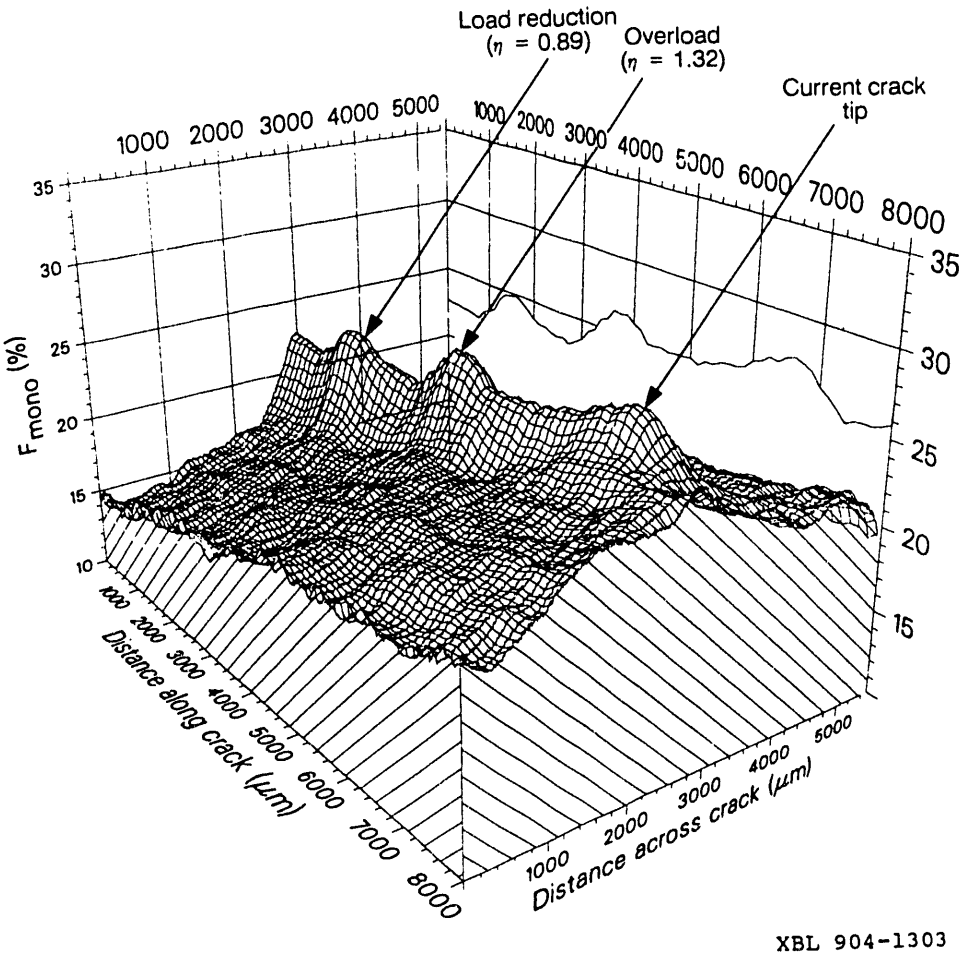

Fig. 8: Morphology of the transformation zone, indicated by the volume fraction of the transformed phase, F_{mono}, derived from Raman spectroscopy measurements, surrounding a fatigue crack in TS-grade Mg-PSZ ($K_c \approx 16$ MPa$\sqrt{m}$), following the loading sequence shown in Fig. 7b [10].

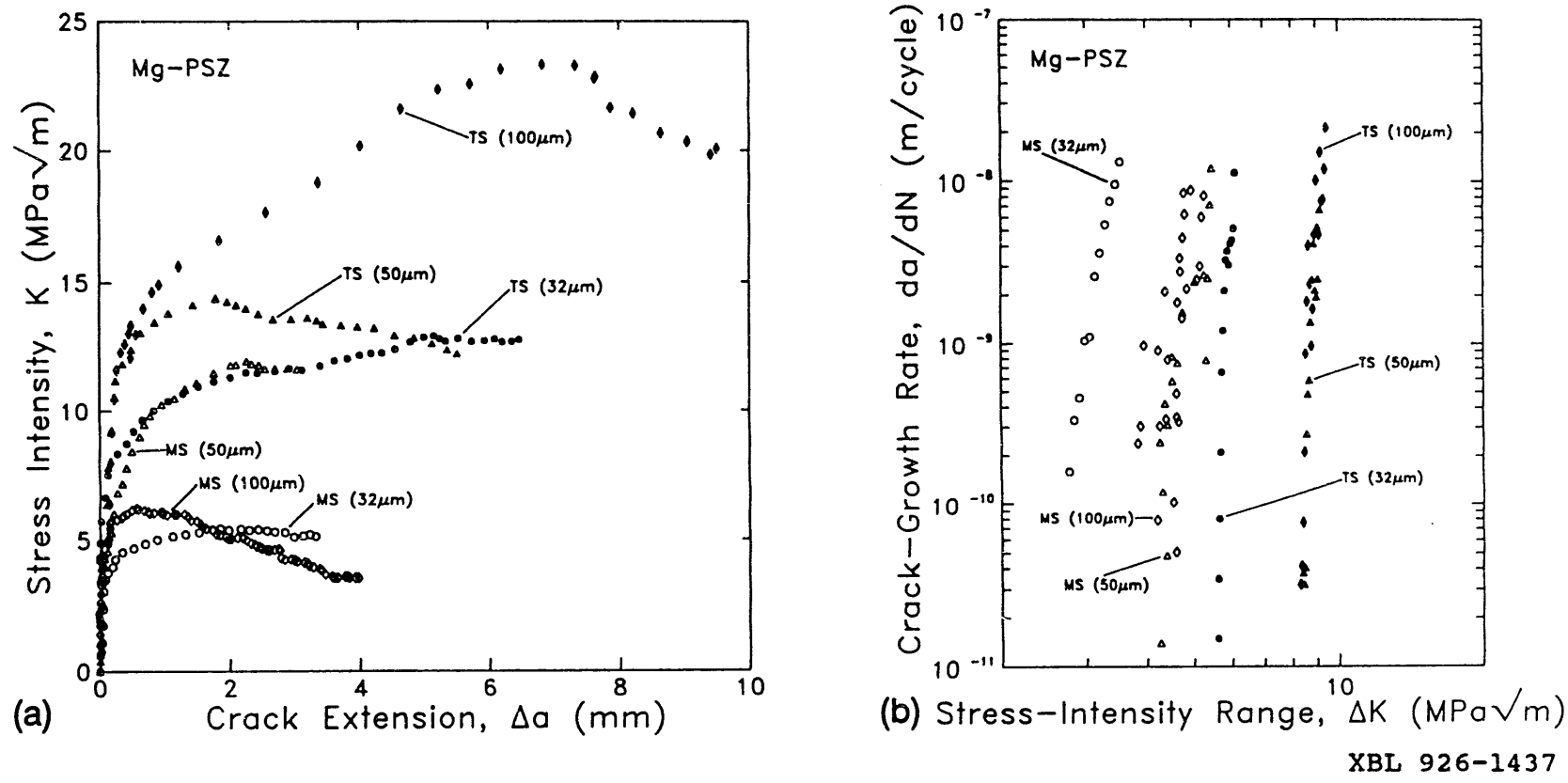

Fig. 9: Effect of grain size (32, 50 and 100 μm) on a) R-curve and b) cyclic fatigue-crack growth behavior (long crack) in MS-grade and TS-grade Mg-PSZ.

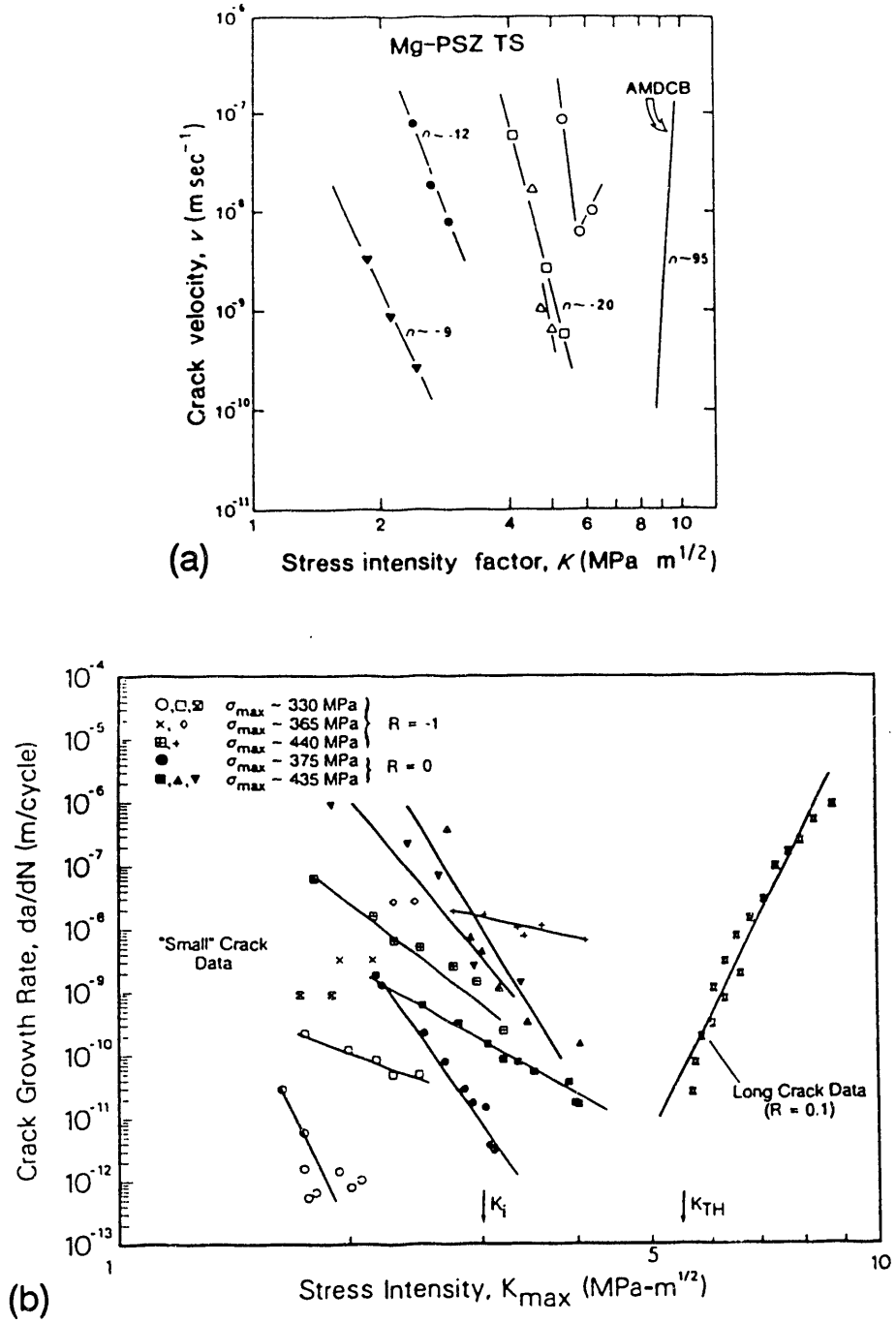

Fig. 10: Small-crack data for MS-grade and TS-grade Mg-PSZ under a) static fatigue [25] and b) cyclic fatigue [15] conditions, showing accelerated small-crack growth rates, occurring below the long-crack threshold, with a negative dependency on the applied stress intensity.

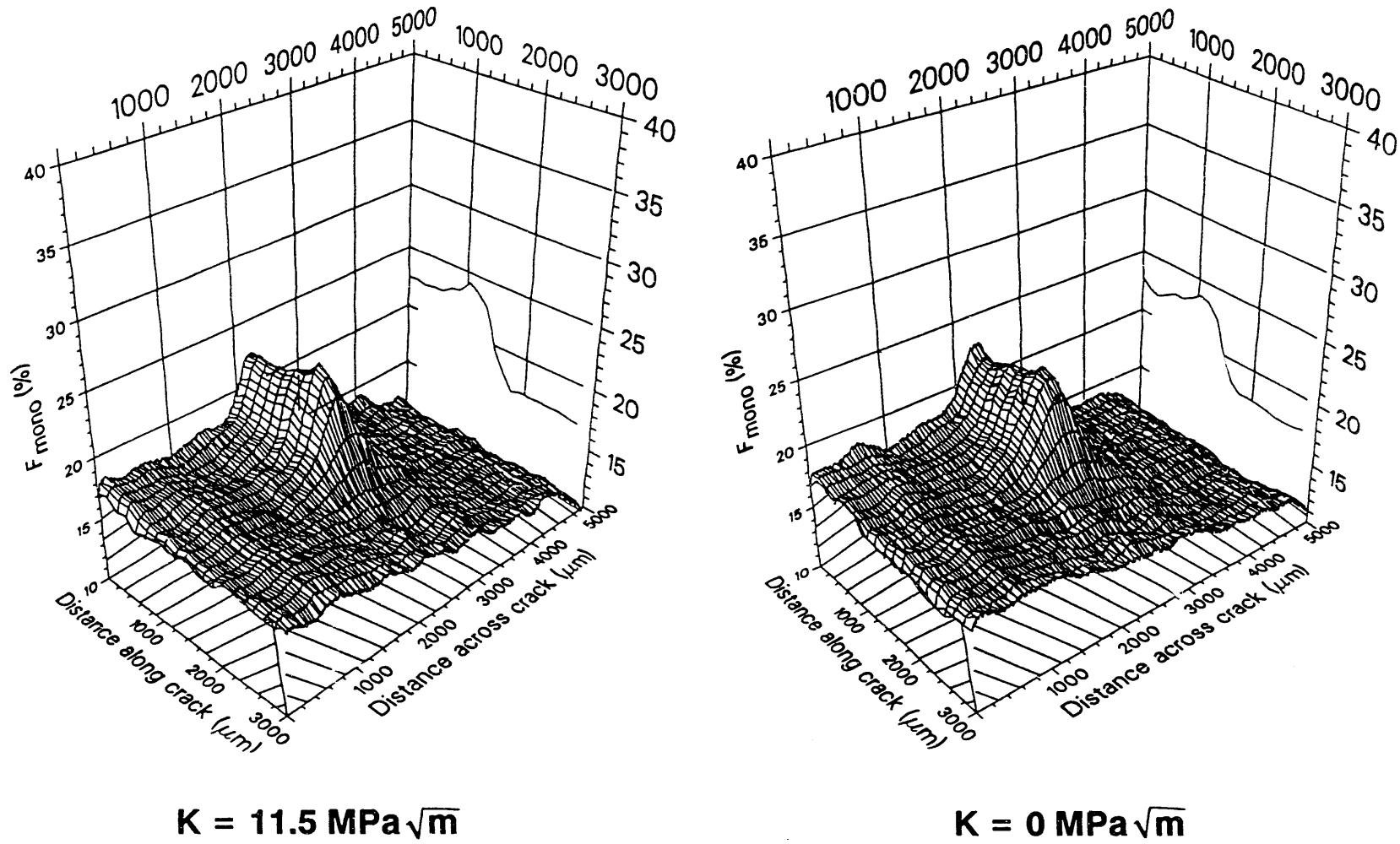

XBL 926-1438

Fig. 11: Transformation zone surrounding a fatigue crack in TS-grade Mg-PSZ *in situ* imaged during a fatigue loading cycle from K_{min} = 0 MPa$\sqrt{m}$ to K_{max} = 11.5 MPa$\sqrt{m}$ using spatially resolved Raman spectroscopy. F_{mono} is the volume fraction of the transformed phase [27]

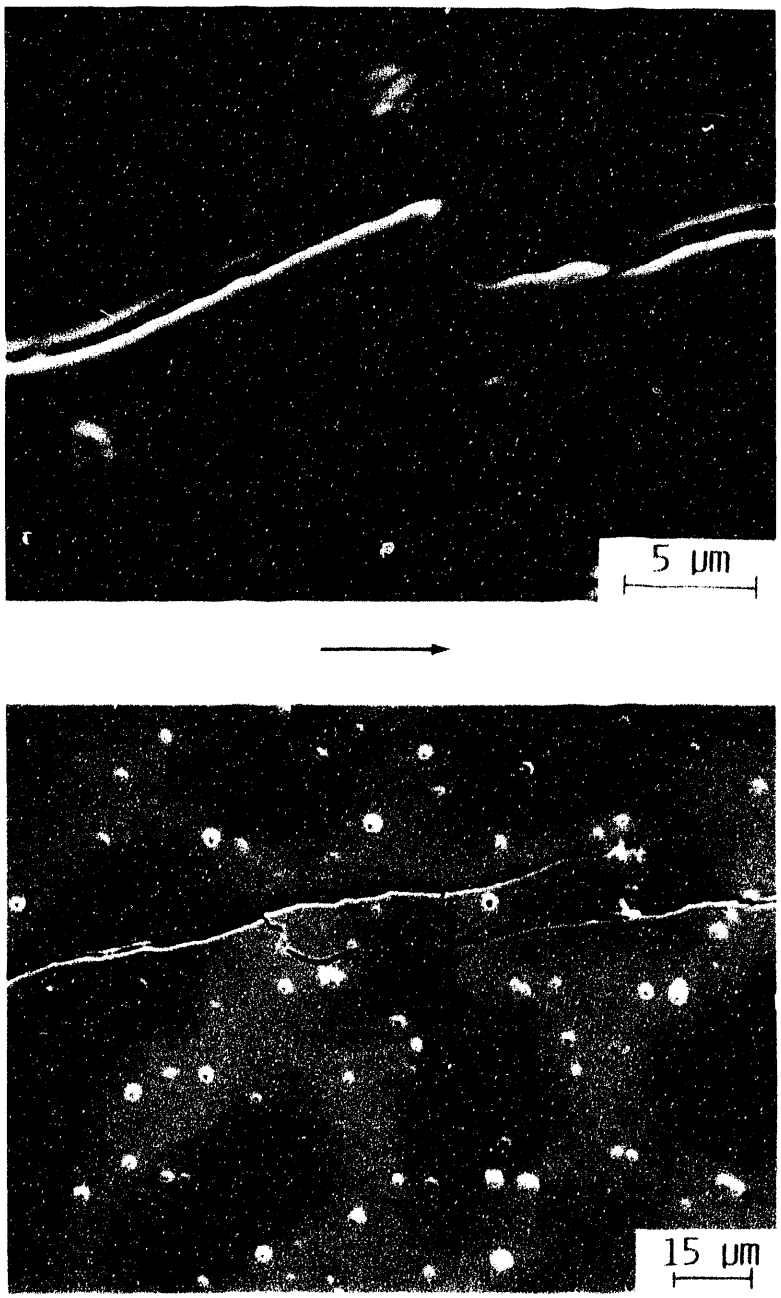

XBB 924-2625

Fig. 12: Examples of uncracked ligament bridges just behind the tip of fatigue cracks in TS-grade Mg-PSZ during cyclic loading.

END

DATE
FILMED
3/1/93